





Cite this: *Dalton Trans.*, 2021, **50**, 4494Received 7th March 2021,  
Accepted 24th March 2021

DOI: 10.1039/d1dt00770j

rsc.li/dalton

## CO<sub>2</sub> activation by permethylpentalene amido zirconium complexes†

Elizabeth A. Hamilton, Alexander F. R. Kilpatrick,  Zoë R. Turner,   
Duncan A. X. Fraser, Jean-Charles Buffet  and Dermot O'Hare \*

We report the synthesis and characterisation of new permethylpentalene zirconium bis(amido) and permethylpentalene zirconium cyclopentadienyl mono(amido) complexes, and their reactivity with carbon dioxide.

### Introduction

The foundations of transition metal amido chemistry were laid in the late 1960s and these compounds are now known to span the largest range of coordination numbers and oxidation states of any in the periodic table.<sup>1</sup> According to the Covalent Bond Classification (CBC) method,<sup>2</sup> the vast majority of terminal amido ligands act as LX ligands and this is indicated by a shorter M–N bond length than the sum of the covalent radii of M and N.<sup>15</sup> Donation of  $\pi$ -electron density from the ligand into partially occupied d-orbitals results in a change of geometry around nitrogen from trigonal pyramidal to planar. In group 4 transition metal(IV) ions, these orbitals are vacant and this allows amido ligands to act as versatile substituents that may impart an extra degree of electronic stabilisation to the electron deficient metal centre. Zirconium forms an extensive range of amido complexes that typically exhibit strong M–N bonds, *ca.* 320–420 kJ mol<sup>-1</sup> in Zr(NR<sub>2</sub>)<sub>4</sub> species. The mean bond strength decreases in the order Zr–O > Zr–Cl > Zr–N > Zr–C.<sup>3</sup>

The O'Hare group has pioneered the organometallic chemistry of permethylpentalene ( $\eta^8$ -C<sub>8</sub>Me<sub>6</sub> = Pn\*), in particular that of the group 4 metals, Ti, Zr and Hf.<sup>4–6</sup> The key entry point for Pn\* zirconium chemistry is {Pn\*Zr( $\mu$ -Cl<sub>3/2</sub>)<sub>2</sub>( $\mu$ -Cl<sub>2</sub>)}·LiTHF,<sup>7</sup> a halide-bridged cluster in which the electron deficiency of a

theoretical 14 VE “Pn\*ZrCl<sub>2</sub>” species is alleviated through dimerisation and incorporation of LiCl. This results in an 18 VE di-zirconium complex with distorted octahedral coordination geometry about each Zr<sup>IV</sup> centre.

The reaction of {Pn\*Zr( $\mu$ -Cl<sub>3/2</sub>)<sub>2</sub>( $\mu$ -Cl<sub>2</sub>)}·LiTHF<sub>x</sub> with LiCp' reagents afforded a series of 18 VE mixed-sandwich complexes, Pn\*ZrCp'Cl, which are highly active precatalysts for ethylene polymerisation.<sup>8,9</sup> The 16 VE bis(allyl) complex, Pn\*Zr( $\eta^3$ -C<sub>3</sub>H<sub>5</sub>)<sub>2</sub>, also obtained by salt metathesis, spontaneously reacts with CO<sub>2</sub> to give the double-insertion product, Pn\*Zr( $\kappa^2$ -O<sub>2</sub>CCH<sub>2</sub>CHCH<sub>2</sub>)<sub>2</sub>, which is 18 VE.<sup>10</sup> To extend our investigation of group 4 Pn\* chemistry we targeted Zr–N bonds in mono and bis-amido Zr complexes and their subsequent insertion reactions with CO<sub>2</sub>.

Reactions of transition metal amides with CO<sub>2</sub> have been known since 1965,<sup>11</sup> and their carbamic acid derivatives, R<sub>2</sub>NCO<sub>2</sub>R', can provide an alternative route to chemicals that are widely used in the pharmaceutical,<sup>12</sup> chemical,<sup>13</sup> and agrochemical industries.<sup>14</sup> This has encouraged significant research into metal complexes for CO<sub>2</sub> activation;<sup>15,16</sup> pentalene ligands have shown the ability to stabilise the highly electropositive metal centres typically required, and recent work has established the reactivity of early transition and f-block metal  $\eta^8$ -pentalene metallocenes with CO<sub>2</sub> and other small molecules.<sup>17–21</sup>

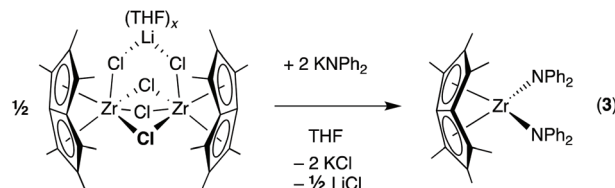
Carbon dioxide insertion reactions into Zr–N bonds to afford zirconium carbamate complexes are limited to a handful of examples.<sup>22</sup> Homoleptic carbamate complexes, Zr( $\kappa^2$ -O<sub>2</sub>CNR<sub>2</sub>)<sub>4</sub>, were obtained by exhaustive carbonation of Zr(NR<sub>2</sub>)<sub>4</sub>,<sup>23–25</sup> and are active precatalysts for the ring-opening polymerisation of *rac*-lactide.<sup>26</sup> Lappert and co-workers synthesised a heteroleptic complex, Cp<sub>2</sub>Zr( $\eta^1$ -OC{O}NMe<sub>2</sub>)(OAR) (Ar = 2,6-C<sub>6</sub>H<sub>3</sub><sup>t</sup>Bu<sub>2</sub>),<sup>27</sup> by carbonation of Cp<sub>2</sub>Zr(NMe<sub>2</sub>)(OAR), however, no X-ray structural data were reported to confirm the suggested monodentate binding mode of the carbamate ligand. Chirik and co-workers reported the reaction of CO<sub>2</sub> with the dimeric *ansa*-zirconocene dinitrogen complex, [Me<sub>2</sub>Si( $\eta^5$ -C<sub>5</sub>Me<sub>4</sub>)( $\eta^5$ -C<sub>5</sub>H<sub>3</sub>{3-<sup>t</sup>Bu})Zr]<sub>2</sub>( $\mu_2$ - $\eta^2$ : $\eta^2$ -N<sub>2</sub>), which resulted in

Chemistry Research Laboratory, Department of Chemistry, University of Oxford, OX1 3TA Oxford, UK. E-mail: Dermot.ohare@chem.ox.ac.uk

† Electronic supplementary information (ESI) available: General details, NMR spectroscopy, X-ray crystallography details. CCDC 2068313–2068316. For ESI and crystallographic data in CIF or other electronic format see DOI: 10.1039/d1dt00770j



$N_2$  carboxylation at each nitrogen atom.<sup>28</sup> Erker and co-workers reported reaction of  $CO_2$  with cationic Zr amido complexes,  $[Cp_2ZrNRR']^+$  (for  $R = R' = Ph$  and  $R = 'Bu, R' = 3,5-(C_6H_3(CH_3)_2)$ , to afford  $[(Cp_2Zr)_2(\mu_2-\kappa^1O,\kappa^1O-O_2CNRR')_2]^{2+}$  species, which show bridging coordination of the carbamate moieties.<sup>29</sup>



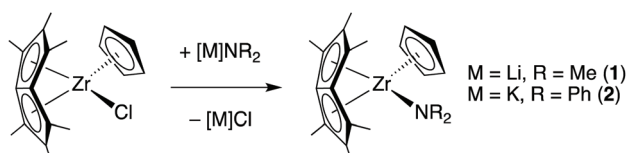
Scheme 2 Synthesis of  $Pn^*Zr$  bis(amido) complex **3**.

## Results and discussion

The reaction of  $Pn^*ZrCpCl$ ,<sup>8</sup> with  $LiNMe_2$  in benzene at room temperature over 3 days afforded a yellow solution and cream precipitate of  $LiCl$  (Scheme 1). Subsequent workup and recrystallisation from hexane at  $-80^\circ C$  furnished a yellow microcrystalline solid of  $Pn^*ZrCp(NMe_2)$  (**1**) in good yield (83%). Similarly, an ampoule was charged with  $Pn^*ZrCpCl$  and  $KNPh_2$  and pre-cooled THF was added at  $-78^\circ C$ . The reaction was allowed to warm to room temperature and stirred for 16 h, which following workup and recrystallisation from a pentane-toluene mixture at  $-80^\circ C$ , furnished the yellow microcrystalline solid  $Pn^*ZrCp(NPh_2)$  (**2**) in 60% yield (Scheme 1). However, the reaction of **2** in benzene required 1.7 equivalents of  $KNPh_2$  for full conversion of  $Pn^*ZrCpCl$  and this resulted in a 63 : 37 mixture of complex **2** and bis(amido) complex  $Pn^*Zr(NPh_2)_2$  (**3**) (*vide infra*).

The identities and purity of **1** and **2** were confirmed by  $^1H$  and  $^{13}C\{^1H\}$  NMR spectroscopy, mass spectrometry, elemental analysis and X-ray crystallography. The  $^1H$  NMR spectra of **1** and **2** show five sharp singlets for the carbocyclic ligands in a 5 : 6 : 6 : 6 integration ratio, which is consistent with  $C_s$  molecular symmetry (Fig. S1†). Three singlets between 1.67–2.11 ppm define the  $Pn^*$ -Me groups, with the wingtip methyl (WT-Me) proton resonance found at a higher chemical shift than the two non-wingtip methyl (NWT-Me) proton resonances. A singlet around 5.50 ppm is assigned in both spectra to protons of the Cp ligand. This lies close to the corresponding resonance in compound  $Pn^*ZrCpCl$  (5.65 ppm) and at a lower chemical shift to the respective resonance in  $PnZrCpCl$  (6.03 ppm).<sup>30</sup> This reflects the increased inductive electron donation resulting from the  $Pn^*$  methyl groups.

The reaction of  $\{Pn^*Zr(\mu-Cl_{3/2})\}_2(\mu-Cl_2)-LiTHF_x$  with  $KNPh_2$  at room temperature resulted in a yellow solution and cream precipitate of  $KCl$  (Scheme 2). Workup and cooling of a hexane solution to  $-80^\circ C$  resulted in the isolation of a yellow microcrystalline solid,  $Pn^*Zr(NPh_2)_2$  (**3**), which was isolated in an 88% yield.



Scheme 1 Synthesis of  $Pn^*Zr$  Cp mono(amido) complexes **1** and **2**.

The  $^1H$  NMR spectrum of **3** displays five signals consistent with solution phase  $C_{2v}$  symmetry (Fig. S2†), which reflects a higher order of symmetry than that found with **1** and **2**. Singlets at 1.77 and 1.87 ppm define the  $Pn^*$  NWT-Me and WT-Me proton environments respectively, whilst resonances in the aromatic region correspond to the protons of the phenyl ring.

Single crystals of **1**, **2** and **3** suitable for X-ray diffraction studies were grown through evaporation of saturated  $C_6D_6$  solutions at room temperature (Fig. 1 and S7†). The solid-state

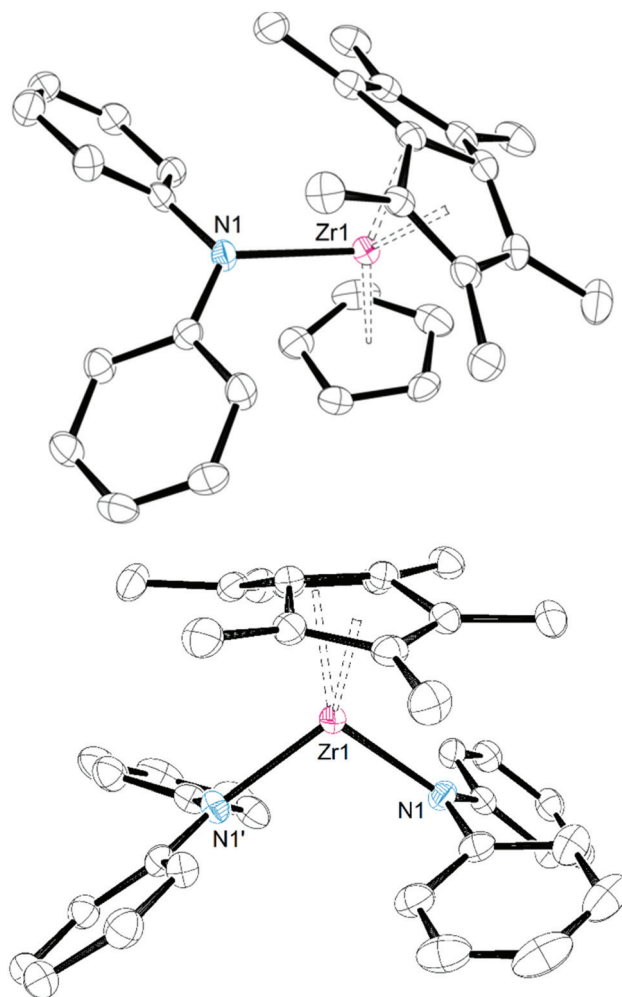


Fig. 1 Solid-state molecular structures of (top)  $Pn^*ZrCp(NPh_2)$  (**2**) and (bottom)  $Pn^*Zr(NPh_2)_2$  (**3**). H atoms are omitted for clarity and thermal ellipsoids are set at 50% probability.



structures of **1** and **2** correspond to  $C_s$  symmetry, in agreement with the solution phase, with a mirror plane that bisects the molecule through the Pn\* bridgehead C–C and Zr–N bonds. By contrast, a descent in symmetry is observed for **3** from  $C_{2v}$  in the solution phase to  $C_2$  in the solid state. This results from the loss of the two vertical mirror planes (one that bisects the Pn\* WT regions and one that runs along the Pn\* bridgehead and Zr–N bonds), which render the NWT–Me resonances equivalent on an NMR timescale. The pentalene fold angles of **1**, **2** and **3** are  $30.58^\circ(13)$ ,  $29.21^\circ(18)$  and  $30.46^\circ(14)$ , respectively (Table 1). These values are similar to pentalene fold angles in {Pn\*Zr( $\mu$ -Cl $_{3/2}$ ) $_2$ ( $\mu$ -Cl $_2$ )-LiTHF $_x$  ( $30.0^\circ$ ) and Pn\*ZrCpCl ( $30.7^\circ$ ),<sup>8</sup> but smaller than those observed in PnZrCpCl ( $33.0^\circ$ ),<sup>30</sup> which may be attributed to the increased donor capability of the Pn\* ligand relative to the unsubstituted pentalene.<sup>31</sup> The angles of N1–Zr–Ct1(Cp)/N1' in **1**, **2** and **3** are found in a similar range to those of Pn\*ZrCpCl ( $103.3^\circ$ ) and PnZrCpCl ( $105.2^\circ$ ),<sup>30</sup> which indicates a distortion from idealised tetrahedral geometry ( $109.5^\circ$ ). C–N–C bond angles around the nitrogen centre are observed to increase from **1** to **2** to **3** ( $112.5(3)^\circ$ ,  $115.5(3)^\circ$  and  $119.0(2)^\circ$ , respectively) and the sum of the bond angles around each nitrogen correspondingly tend towards to  $360^\circ$  ( $351.2^\circ$ ,  $357.4^\circ$  and  $359.8^\circ$  respectively). This is attributed to a shift towards  $sp^2$  hybridisation, as the planar arrangement allows for more effective donation of the  $\pi$ -electron density from the N 2p-orbitals to unoccupied Zr 4d-orbitals. For **1** and **2** to be 18 VE complexes the amido ligand would be required to act as a  $1e^-$  donor, with corresponding  $sp^3$  hybridisation around the nitrogen atom. By contrast in **3**, it can be rationalised that substitution of a  $5e^-$  donating Cp ligand for a second amido ligand requires both nitrogen atoms to act as  $3e^-$  donors in order to maintain a 18 VE configuration, which requires  $sp^2$  hybridisation.<sup>32,33</sup> Although changes in hapticity of bound pentalene ligands have been reported, these are extremely rare. One example by Kilpatrick *et al.* in a titanium bis(oxo) bridged dimer observed a change in hapticity of the pentalene ligand from  $\eta^8$ - to  $\eta^5$ -mode upon addition of pyridine.<sup>17</sup>

Bearing in mind the background outlined in the introduction, the potential of **1**, **2** and **3** to activate CO $_2$  was investigated. A frozen solution of **1** in C $_6$ D $_6$  under static vacuum was exposed to an atmosphere of CO $_2$  (1 bar overpressure) at  $-78^\circ\text{C}$ . The reaction mixture was allowed to warm to room temperature and this resulted in an almost instant quantitative conversion of **1** to Pn\*ZrCp( $\eta^1$ -O $_2$ CNMe $_2$ ) (**4**; eqn (S1)†) analogous to the synthesis of M(O $_2$ CNMe $_2$ ) $_4$  (M = Ti, Zr, V).<sup>23,24</sup>

**Table 1** X-ray crystallographic parameters, bond lengths (Å) and angles (°) for complexes **1**, **2** and **3**

	<b>1</b>	<b>2</b>	<b>3</b>
Zr–N1	2.136(3)	2.236(3)	2.188(2)
Zr–Ct1(Cp)/N1'	2.280(3)	2.2484(17)	2.1191(12)
Zr–Ct2(Pn*)	2.1326(12)	2.1290(14)	2.1191(12)
Zr–Ct3(Pn*)	2.1254(4)	2.1377(18)	2.188(2)
N1–Zr–Ct1(Cp)/N1'	103.77(10)	102.45(9)	107.57(12)
Fold angle	30.58(13)	29.21(18)	30.46(14)

However, by comparison the analogous addition of CO $_2$  to a frozen solution of **2** in C $_6$ D $_6$  did not yield a reaction, despite heating at  $75^\circ\text{C}$  for 16 h.

The generally accepted mechanism for d-block metals involves a direct nucleophilic attack of the metal-coordinated nitrogen to carbon dioxide, with the generation of an intermediate N-bound carbamate/carbamic acid moiety.<sup>22</sup> Subsequent rearrangement provides the typical O-coordinated carbamate ligand. The facile reaction of **1** with CO $_2$  to afford **4**, compared with no reaction observed with **2** and CO $_2$  can be explained by the lower Lewis basicity of HNPh $_2$  compared with HNMe $_2$ . Furthermore, the increased steric congestion around the Zr–N bond in **2** may further retard CO $_2$  insertion.

Complex **4** was characterised by NMR and IR spectroscopy, elemental analysis and mass spectrometry. The  $^1\text{H}$  NMR spectrum revealed singlets at 1.88, 1.98 and 2.09 ppm, which define the Pn\*–Me groups (Fig. S3†). These data are in agreement with **4** possessing  $C_s$  symmetry in the solution phase, whereby a mirror plane is found bisecting the Pn\* bridgehead, Zr–O and Zr–Cp bonds, with the result of one Pn\*–Me NWT and two Pn\*–WT environments. Singlets at 2.52 ppm and 5.81 ppm were assigned to protons of the NMe $_2$  and Cp ligands respectively. These resonances tend to lie at a higher chemical shifts than the corresponding peaks in the starting material **1** (1.84, 1.90, 2.11, 2.41 and 5.73 ppm respectively), which is attributed to electron withdrawing effect of the carbamate ligand in **4**. The  $^{13}\text{C}\{^1\text{H}\}$  NMR spectrum is consistent with this structure and the characteristic carbamate resonance is located at 166.7 ppm. This demonstrates a contrast between the carbamate and carboxylate moieties the additional contribution of electron density by the nitrogen atom results in a reduced chemical shift with respect to the corresponding peak in carboxylate species Pn\*Ti( $\kappa^2$ -O $_2$ CCH $_2$ SiMe $_3$ ) $_2$  (189.8 ppm), Pn\*Ti( $\kappa^2$ -O $_2$ CCH $_2$ <sup>t</sup>Bu) $_2$  (189.9 ppm),<sup>19</sup> and Pn\*ZrCp( $\eta^1$ -O $_2$ CC $_3$ H $_5$ ) (188.0 ppm).<sup>10</sup> IR spectroscopy of **4** reveals strong  $\nu_a(\text{CO})$  and  $\nu_s(\text{CO})$  stretches at values at 1564 and 1408  $\text{cm}^{-1}$ , respectively. A key determinant in the bonding mode is the difference between these two frequencies compared to the corresponding value of the free carboxylate ion, 164  $\text{cm}^{-1}$ .<sup>34,35</sup> The observed difference of 156  $\text{cm}^{-1}$  suggests monodentate coordination, in accordance with stretches reported for one of the few reported examples of the Zr( $\eta^1$ -O $_2$ CNMe $_2$ ) bonding motif in the literature.<sup>27</sup>

The synthesis of Pn\*Zr( $\kappa^2$ -O $_2$ CNPh $_2$ ) $_2$  (**5**) was achieved by the addition of CO $_2$  (1 bar overpressure) to a frozen solution of **3** at  $-78^\circ\text{C}$ . Following work-up and recrystallisation from benzene- $d_6$ , complex **5** was isolated as a white solid in 70% yield (eqn (S2)†). This bidentate CO $_2$  bonding mode is expected to provide enhanced electronic stability in **5**, relative to the monodentate binding found in **4**.<sup>36</sup> The proposed formulation of **5** is consistent with data from NMR and IR spectroscopy, mass spectrometry, elemental analysis and a single-crystal X-ray diffraction study. The  $^1\text{H}$  NMR spectrum of the bis(carbamate) complex **5** shows three resonances in the aliphatic region (1.92, 2.03 and 2.08 ppm), in contrast to the two CH $_3$  resonances observed in the starting material **3** (1.77 and



1.87 ppm; Fig. S4†). This reflects a decrease in symmetry on the NMR timescale from the  $C_{2v}$  to the  $C_2$  point group. As with **4**, both the aliphatic and aromatic NMR signals of **5** are deshielded with respect to the corresponding signals in the starting complex **3**. The  $^{13}\text{C}\{^1\text{H}\}$  NMR spectrum reflects the reduced symmetry, with three  $\text{Pn}^*\text{-Me}$  carbon environments observed compared to the two found in the solution phase of **3**. The bridgehead carbons are found to be equivalent (128.9 ppm), a diagnostic feature for differentiation between  $C_2$  and  $C_s$  symmetric  $\text{Pn}^*$  complexes. A singlet carbamate resonance frequency is observed at the highest chemical shift, 167.6 ppm, which is in close agreement with **4**, but slightly below that reported (179.8 ppm) for the similar bidentate complex  $\text{Pn}^*\text{Zr}\{\kappa^2\text{-(O}_2\text{CCH}_2\text{CHCH}_2)\}_2$ . Mesomeric donation is reflected in the IR spectrum of **5**, which shows characteristic bands at 1513 and 1422  $\text{cm}^{-1}$  assigned to the  $\nu_{\text{as}}(\text{CO})$  and  $\nu_{\text{s}}(\text{CO})$  carbamate stretches respectively. The separation of these stretching frequencies is significantly less than that observed both in the free ion<sup>35</sup> and **4** and is consistent with bidentate coordination.

A single crystal X-ray diffraction study of **5** confirmed the bidentate coordination mode of the two carbamate ligands (Fig. 2) giving  $C_2$  molecular symmetry, in agreement with the solution phase. Each  $\text{CO}_2$  molecule inserts to give a four-membered  $\text{Zr-O-C-O}$  ring, which lies in the same plane as its corresponding nitrogen atom. The sum of the angles around the C and N nitrogen atoms total to exactly  $360^\circ$ , further corroborating the  $\text{sp}^2$  hybridisation of the atoms. This heterometal-lacycle motif is known in other carbamates<sup>37</sup> and suggests added stability from the overlapping  $\pi$ -orbitals. Though no bis(Cp) zirconium complexes with a chelating  $\kappa^2$ -carbamate ligand have been structurally characterised, comparisons can be made between **5** and the heteroleptic and mono(Cp) diethylcarbamate complexes,  $\text{Zr}(\kappa^2\text{-O}_2\text{CNEt}_2)_4$  and  $\text{CpZr}(\kappa^2\text{-O}_2\text{CNEt}_2)_3$  (Table S1†).<sup>25</sup> The average  $\text{Zr-O}$  bond is observed to be marginally longer in **5** (2.239(4) Å) than in  $\text{Zr}(\kappa^2\text{-O}_2\text{CNEt}_2)_4$

(2.201(2) Å) and  $\text{CpZr}(\kappa^2\text{-O}_2\text{CNEt}_2)_3$  (2.226(3) Å), attributed to the increased bulk of the  $\text{Pn}^*$  ligand and its enhanced electron donating abilities.

## Conclusions

The synthesis and full characterisation of the first mono(amido)  $\text{Pn}^*\text{Zr}$  complexes,  $\text{Pn}^*\text{ZrCp}(\text{NR}_2)$  ( $\text{R} = \text{Me}, \text{Ph}$ ), and the first bis(amido)  $\text{Pn}^*\text{Zr}$  complex,  $\text{Pn}^*\text{Zr}(\text{NPh}_2)_2$ , have been reported. The amido ligands show interesting versatility in their bonding, acting as both  $1e^-$  and  $3e^-$  donors to accommodate the electronic requirements of the metal centre. Multiple variants of the amido alkyl substituents have been attempted and it has been observed that whilst small groups encourage dimerisation, larger groups inhibit reactivity. A steric compromise is therefore required to afford the monometallic species.

The zirconium amido species  $\text{Pn}^*\text{ZrCp}(\text{NR}_2)$  ( $\text{R} = \text{Me}$  (**1**),  $\text{Ph}$  (**2**)) and  $\text{Pn}^*\text{Zr}(\text{NPh}_2)_2$  (**3**) were tested for their reactivity with  $\text{CO}_2$ . This proceeds *via* insertion of the  $\text{CO}_2$  molecule into the  $\text{Zr-N}$  bonds resulting in the formation of the carbamate complexes  $\text{Pn}^*\text{ZrCp}(\eta^1\text{-O}_2\text{CNMe}_2)$  (**4**) and  $\text{Pn}^*\text{Zr}(\kappa^2\text{-O}_2\text{CNPh}_2)_2$  (**5**), respectively. Although both a (Cp)( $\text{NR}_2$ ) and a ( $\text{NR}_2$ )<sub>2</sub> ligand set donate  $6e^-$  in total, the Cp has a larger steric demand than an amide. Hence, the reactivity of (Cp)( $\text{NPh}_2$ ) is hampered due to the reduced nucleophilicity of the amide (since **1** reacts) and the increased steric protection of the Cp (since **3** reacts) and both factors prevent carboxylation of complex **2**. These results demonstrate the versatility of amido and carbamate as ligands in adapting to the electronic requirements of the metal centre, and further illustrate the ability of  $\text{Pn}^*$  metallocenes to activate small molecules.

## Conflicts of interest

There are no conflicts to declare.

## Acknowledgements

A.F.R.K., Z.R.T. (SCG Fellowship), D.A.X.F. and J.-C.B. would like to thank SCG Chemicals Co. Ltd (Thailand) for funding and Chemical Crystallography (University of Oxford) for use of the single crystal diffraction instrumentation.

## Notes and references

- M. Lappert, A. Protchenko, P. Power and A. Seeber, *Metal amide chemistry*, John Wiley & Sons, 2008.
- M. Green, *J. Organomet. Chem.*, 1995, **500**, 127–148.
- M. F. Lappert, D. S. Patil and J. B. Pedley, *J. Chem. Soc., Chem. Commun.*, 1975, 830–831.
- A. E. Ashley, A. R. Cowley and D. O'Hare, *Chem. Commun.*, 2007, 1512–1514.

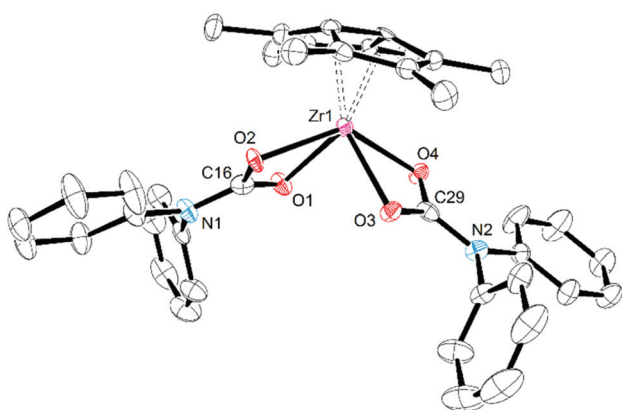


**Fig. 2** Solid-state molecular structure of  $\text{Pn}^*\text{Zr}(\kappa^2\text{-O}_2\text{CNPh}_2)_2$  (**5**). H atoms are omitted for clarity and thermal ellipsoids are set at 50% probability. Selected bond lengths/Å and angles/ $^\circ$ :  $\text{Zr1-O1}$  2.258(4),  $\text{Zr1-O2}$  2.223(4),  $\text{Zr1-O3}$  2.250(4),  $\text{Zr1-O4}$  2.223(4),  $\text{N1-C16}$  1.376(8),  $\text{N2-C29}$  1.366(8).



- 5 F. G. N. Cloke, J. C. Green, A. F. R. Kilpatrick and D. O'Hare, *Coord. Chem. Rev.*, 2017, **344**, 238–262 and references therein.
- 6 D. D. Clement, S. C. Binding, T. A. Q. Arnold, F. M. Chadwick, I. J. Casely, Z. R. Turner, J.-C. Buffet and D. O'Hare, *Polyhedron*, 2019, **157**, 146–151.
- 7 R. T. Cooper, F. M. Chadwick, A. E. Ashley and D. O'Hare, *Organometallics*, 2013, **32**, 2228–2233.
- 8 F. M. Chadwick, R. T. Cooper, A. E. Ashley, J.-C. Buffet and D. O'Hare, *Organometallics*, 2014, **33**, 3775–3785.
- 9 D. A. X. Fraser, Z. R. Turner, J.-C. Buffet and D. O'Hare, *Organometallics*, 2016, **35**, 2664–2674.
- 10 F. M. Chadwick, R. T. Cooper and D. O'Hare, *Organometallics*, 2016, **35**, 2092–2100.
- 11 G. Chandra and M. F. Lappert, *Inorg. Nucl. Chem. Lett.*, 1965, **1**, 83–84.
- 12 J. Barthelemy, *Lyon Pharm.*, 1986, **37**, 249–263.
- 13 M. Aresta and E. Quaranta, *Chemtech*, 1997, **27**, 32–40.
- 14 T. T. Wu, J. Huang, N. D. Arrington and G. M. Dill, *J. Agric. Food Chem.*, 1987, **35**, 817–823.
- 15 D. B. Dell'Amico, F. Calderazzo, L. Labella, F. Marchetti and G. Pampaloni, *Chem. Rev.*, 2003, **103**, 3857–3898.
- 16 M. Aresta, A. Dibenedetto and A. Angelini, *Chem. Rev.*, 2014, **114**, 1709–1742.
- 17 A. F. R. Kilpatrick and F. G. N. Cloke, *Chem. Commun.*, 2014, **50**, 2769–2771.
- 18 A. F. R. Kilpatrick, J. C. Green and F. G. N. Cloke, *Organometallics*, 2015, **34**, 4816–4829.
- 19 R. T. Cooper, F. M. Chadwick, A. E. Ashley and D. O'Hare, *Chem. Commun.*, 2015, **51**, 11856–11859.
- 20 N. Tsoureas, J. Green, F. G. N. Cloke, H. Puschmann, M. Roe and G. J. Tizzard, *Chem. Sci.*, 2018, **9**, 5008–5014.
- 21 N. Tsoureas, L. Maron, A. F. R. Kilpatrick, R. A. Layfield and F. G. N. Cloke, *J. Am. Chem. Soc.*, 2019, **142**, 89–92.
- 22 G. Bresciani, L. Biancalana, G. Pampaloni and F. Marchetti, *Molecules*, 2020, **25**, 3603.
- 23 M. H. Chisholm and M. W. Extine, *J. Am. Chem. Soc.*, 1977, **99**, 792–802.
- 24 M. H. Chisholm and M. W. Extine, *J. Am. Chem. Soc.*, 1977, **99**, 782–792.
- 25 F. Calderazzo, U. Englert, C. Maichle-Mössmer, F. Marchetti, G. Pampaloni, D. Petroni, C. Pinzino, J. Strähle and G. Tripepi, *Inorg. Chim. Acta*, 1998, **270**, 177–188.
- 26 F. Marchetti, G. Pampaloni, C. Pinzino, F. Renili, T. Repo and S. Vuorinen, *Dalton Trans.*, 2013, **42**, 2792–2802.
- 27 A. W. Duff, R. A. Kamarudin, M. F. Lappert and R. J. Norton, *J. Chem. Soc., Dalton Trans.*, 1986, 489–498.
- 28 D. J. Knobloch, H. E. Toomey and P. J. Chirik, *J. Am. Chem. Soc.*, 2008, **130**, 4248–4249.
- 29 A. T. Normand, C. G. Daniliuc, B. Wibbeling, G. Kehr, P. Le Gendre and G. Erker, *J. Am. Chem. Soc.*, 2015, **137**, 10796–10808.
- 30 K. Jonas, P. Kolb, G. Kollbach and B. Gabor, *Angew. Chem., Int. Ed.*, 1997, **36**, 1714–1718.
- 31 F. G. N. Cloke, P. B. Hitchcock, M. C. Kuchta and N. A. Morley-Smith, *Polyhedron*, 2004, **23**, 2625–2630.
- 32 E. Hey-Hawkins, *Chem. Rev.*, 1994, **94**, 1661–1717.
- 33 D. M. P. Mingos, *J. Organomet. Chem.*, 2004, **689**, 4420–4436.
- 34 G. Deacon and R. J. Phillips, *Coord. Chem. Rev.*, 1980, **33**, 227–250.
- 35 K. Ito and H. J. Bernstein, *Can. J. Chem.*, 1956, **34**, 170–178.
- 36 P. Braunstein and D. Nobel, *Chem. Rev.*, 1989, **89**, 1927–1945.
- 37 J. A. Higgins Frey, F. G. N. Cloke and S. M. Roe, *Organometallics*, 2015, **34**, 2102–2105.

